Int. J. Peptide Protein Res. 23, 1984, 1–24

Vibrational analysis of peptides, polypeptides, and proteins

XVII. Normal modes of crystalline Pro-Leu-Gly-NH_2, a type II β-turn

VAMAN M. NAIK and S. KRIMM

Biophysics Research Division, The University of Michigan, Ann Arbor, Michigan, USA

Received 8 February, accepted for publication 4 May 1983

A normal mode calculation has been done for Pro-Leu-Gly-NH_2 in its crystalline type II β-turn structure, and assignments have been made to infrared and Raman bands of this molecule and its *N*-deuterated derivative. Observed and calculated frequencies below 1700 cm^{-1} agree to within about 6 cm^{-1}. This analysis provides a sound basis for studying the conformation dependence of the vibrational spectrum.

Key words: β-turns; infrared spectra; melanocyte stimulating hormone; normal mode calculation; Raman spectra

Vibrational spectroscopic analysis, namely infrared (i.r.) and Raman spectra combined with normal mode calculations, can be a powerful tool in studying the conformation of peptide molecules. In earlier studies on β-turns (1,2) we showed, by calculations on canonical structures, that the amide I, II, III, and V frequencies could be used to characterize type I, II, and III β-turns (3). When tested on known β-turn structures, both in the tetrapeptide Z-Gly-Pro-Leu-OH (4) and in the protein insulin (5), such calculations gave good agreement with observed frequencies. This approach is particularly powerful in discriminating between β-turn structures suggested by conformational energy calculations, as was shown by our studies on cyclo (L-Ala-Gly-Aca) (6) and cyclo (L-Ala-L[D]-Ala-Aca) (7). We therefore expect that normal mode analysis should provide a deeper insight into β-turn conformation than would otherwise be possible.

We have now extended such an analysis to the tripeptide Pro-Leu-Gly-NH_2. This peptide is the *C*-terminal tripeptide of oxytocin, which is known to be an inhibiting factor for the release of pituitary melanotropin (melanocyte stimulating hormone) (8,9). X-ray crystallographic studies on this peptide show that it has a type II β-turn structure in the crystal (10). Raman spectra in the solid state have been studied (11), as well as Raman (11, 12), n.m.r. (13–15), and CD (16) spectra in solution, but no detailed vibrational analysis has been reported. A preliminary summary has been given of our earlier work (17).

EXPERIMENTAL PROCEDURES

The Pro-Leu-Gly-NH_2 was obtained from the Protein Research Foundation of Japan. It was crystalline and gave Raman spectra similar to those reported earlier (11, 12) for material on which the X-ray analysis was done (10), thus establishing that our conformation is that found in the crystal (10). The molecule was deuterated by dissolving in D_2O for ~36 h and

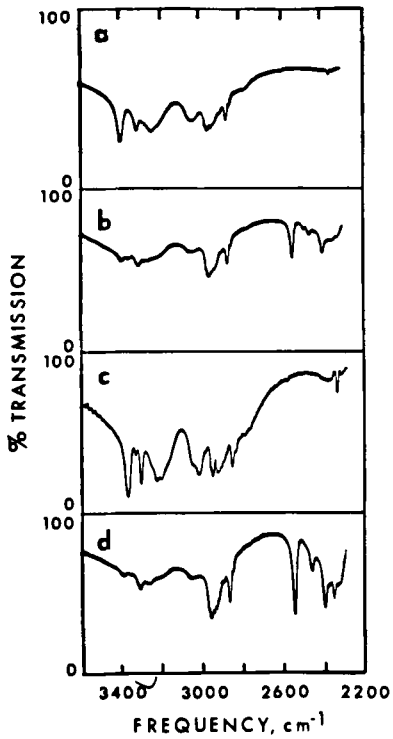

FIGURE 1

Infrared spectra in the 2200–3600 cm^{-1} region of crystalline Pro-Leu-Gly-NH_2, (a) at room temperature and (c) at liquid N_2 temperature; and of its *N*-deuterated derivative, (b) at room temperature and (d) at liquid N_2 temperature.

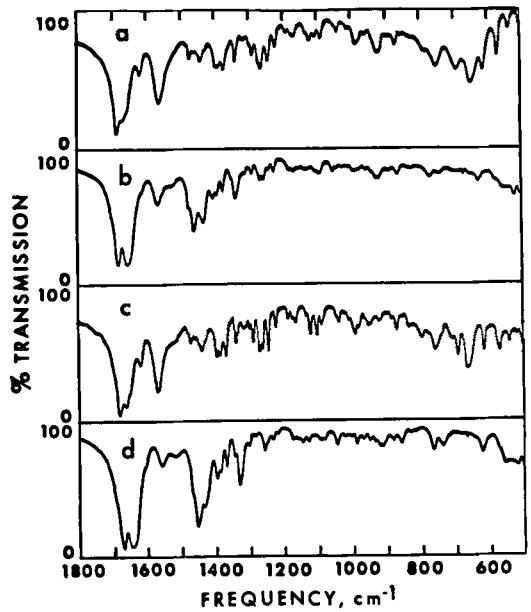

FIGURE 2

Infrared spectra in the 500–1800 cm^{-1} region of crystalline Pro-Leu-Gly-NH_2, (a) at room temperature and (c) at liquid N_2 temperature; and of its *N*-deuterated derivative, (b) at room temperature and (d) at liquid N_2 temperature.

then freeze drying. Infrared spectra were obtained in KBr disks, at room and liquid N_2 temperatures, on a Perkin-Elmer 180 Spectrophotometer, and these are shown in Figs. 1 and 2. Raman spectra were also recorded at these temperatures, using a spectrometer described previously (18) to which data acquisition capabilities (Cromemco Z-2 microcomputer system) had been added. The room and liquid N_2 temperature spectra are shown in Figs. 3 and 4. These were obtained with 514.5 nm line excitation and a spectral band width of $\sim 1\ cm^{-1}$. The estimated accuracy of sharp bands is $1-2\ cm^{-1}$.

NORMAL MODE CALCULATION

The conformational angles of Pro-Leu-Gly-NH_2, taken from the X-ray analysis (10), are: ψ_1(Pro) $= 152.9°$, ϕ_2(Leu) $= -61.2°$, ψ_2(Leu) $= 127.8°$, and ϕ_3(Gly) $= 71.8°$. These are close to the "standard" values of the dihedral angles of a type II β-turn (3), viz. $(\phi, \psi)_2 = -60°, 120°$ and $\phi_3 = 80°$. In the X-ray work (10) hydrogen atom positions were not refined, and there was considerable variation in the bond lengths and angles. In our calculation we used the same structural parameters as in our previous studies (19, 20). Also, all of the peptide units were taken as planar, even though the peptide bond between Pro and Leu is found to deviate by 9° from planarity (10). A schematic view of the structure is shown in Fig. 5. One H_2O molecule is shared by two Pro-Leu-Gly-NH_2 molecules (10), the O atom of the H_2O being bonded to the NH of Gly (r(N . . . O) = 2.98 Å) and an OH bond of H_2O being bonded to the N of Pro (r(N . . . O) = 2.79 Å).

The internal and local symmetry coordinates for the peptide moiety were defined as in our earlier work (19). The NH_2 wagging coordinate of the trigonal planar CNH_2 group was defined

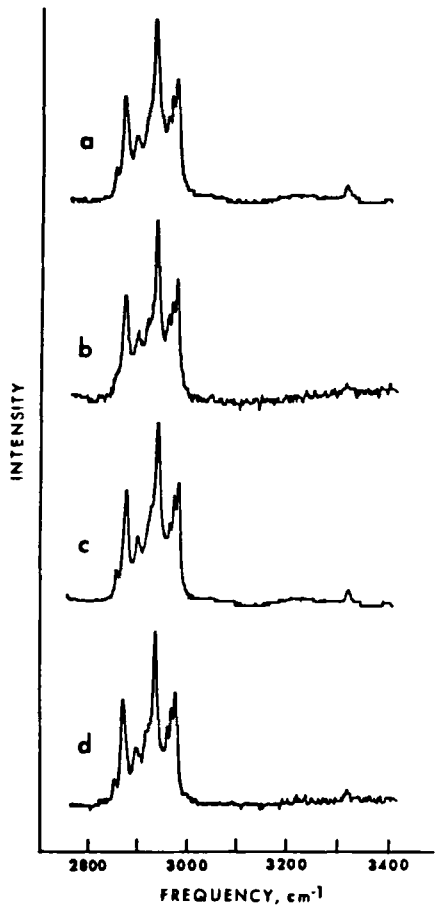

FIGURE 3

Raman spectra in the 2700–3400 cm^{-1} region of crystalline Pro-Leu-Gly-NH_2, (a) at room temperature and (c) at liquid N_2 temperature; and of its *N*-deuterated derivative, (b) at room temperature and (d) at liquid N_2 temperature.

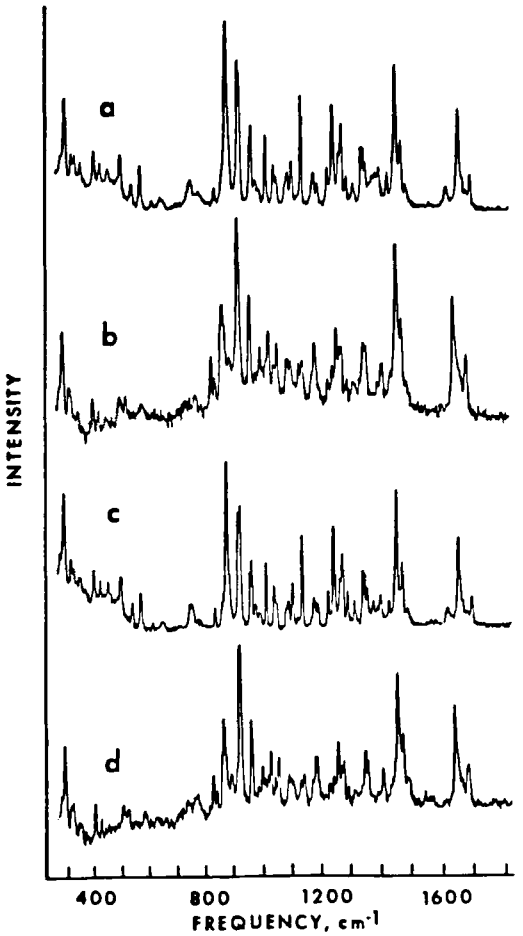

FIGURE 4

Raman spectra in the 300–1800 cm^{-1} region of crystalline Pro-Leu-Gly-NH_2 (a) at room temperature and (c) at liquid N_2 temperature; and of its *N*-deuterated derivative, (b) at room temperature and (d) at liquid N_2 temperature.

as an out-of-plane bend by $\Delta\omega = \Delta\alpha_C \sin$ (HNH), where $\Delta\alpha_C$ is the displacement of the CN bond from the HNH plane.

The peptide force field used in the present calculation was taken from those for poly (glycine I) (21), β-poly(L-alanine) (22), and poly(L-proline)(23). Additional force constants were required for the prolyl ring, the leucyl side chain, and the $CONH_2$ end group, and these are given in Table 1. For the prolyl ring, the intramolecular force constants associated with the NH group were transferred from β-poly(L-alanine (22). While this is somewhat arbitrary, the complex NH stretching region of the spectrum does not at present permit an analysis in great detail. The force constants selected for the HOH . . . N (Pro) hydrogen bond are really estimates at this point, but these will affect mainly the very low frequencies. For the leucyl side chain, the force constants were transferred from β-poly(L-alanine) (22) and from work on hydrocarbons (24). For the $CONH_2$ group, a Urey-Bradley force field for acetamide (25, 26)

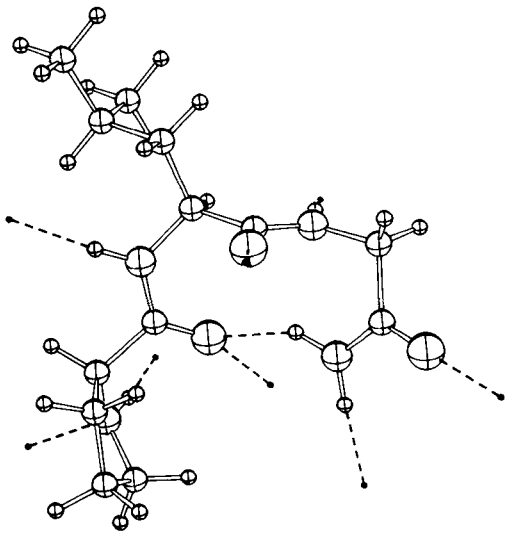

FIGURE 5

Structure of crystalline Pro-Leu-Gly-NH_2. Broken lines are hydrogen bonds; small circles are locations of external oxygen or hydrogen atoms bonded to NH or CO groups, respectively.

was converted to a valence force field and the relevant force constants were transferred to Pro-Leu-Gly-NH_2. Of these, f(CNH) was lowered from 0.700 to 0.590 mdyn·Å in order to give agreement with the lower observed NH_2 bend frequency (1615 cm^{-1}) than in acetamide (1640 cm^{-1}). This also helps to account for the lower NH_2 rock (1135 (R) and 1130 (i.r.) vs. 1154 cm^{-1} in acetamide) and higher NH_2 (i.e. CN(T)) torsion (868 (i.r.) vs. 810 cm^{-1}) frequencies. Such a change is reasonable for Pro-Leu-Gly-NH_2 since we have included hydrogen bonds for both NH bonds of the NH_2 group. The NH_2 wag force constant was increased from 0.089 to 0.140 mdyn·Å in order to reproduce the NH_2 wag frequency at ~ 745 cm^{-1} (this mode is found at 700 cm^{-1} in acetamide).

In addition to the intramolecular hydrogen bond, external hydrogen bonds were included for all NH and CO groups as was done before (1), namely by bonding an O atom to an NH group and an H atom to a CO group. All f(O ... H) force constants were obtained by interpolation or extrapolation from the values for poly(glycine I) (21) and β-poly(L-alanine) (22), using the actual r(N ... O) distances from the crystal structure (10). Transition dipole coupling (27, 28) was included for amide I ($\Delta\mu_{eff}$ = 0.37D) and amide II ($\Delta\mu_{eff}$ = 0.29D) modes.

RESULTS AND DISCUSSION

The observed (room temperature) and calculated frequencies of Pro-Leu-Gly-NH_2 and its *N*-deuterated derivative are given in Tables 2 and 3, respectively. The calculations indicate that there is strong mixing of internal coordinates throughout the molecule; for this reason all the contributions to the potential energy equal to or greater than 5% are included in Tables 2 and 3.

The NH stretch region is complex, both because of the presence of NH_2 and NH groups (prolyl and peptide) as well as the contributions due to Fermi resonance between fundamentals and overtones and combinations of NH bend modes. We will, therefore, not analyze this region in great detail at the present time. The NH_2 antisymmetric stretch (3389W, R and 3395 VS, i.r.) and NH_2 symmetric stretch (3235 VW, R and 3240S, i.r.) modes are in good agreement with similar bands found in acetamide (25). At low temperature the i.r. bands shift down, the former to 3376 cm^{-1} and the latter to (probably) 3214 cm^{-1} (a new band emerges at 3244 cm^{-1}). This probably is a result of the stronger hydrogen bonds formed by this group when the unit cell contracts.

The amide A NH stretch modes are assignable to observed i.r. bands at 3314 MS and 3240 S cm^{-1} (3312 and 3244 cm^{-1} at low temperature) but the specific groups involved are less certain at present. Because r(N ... O) of Gly (2.98 Å) is larger than r(N ... O) of Leu (2.85 Å), we expect the frequency of NH(G) to be higher than that of NH(L). The NH stretch in saturated ring molecules is found in the region of 3280–3290 cm^{-1} (29) (e.g. pyrrolidone – 3280, 2,5-dimethylpyrrolidone – 3290, piperidine – 3285, all as neat liquids), and the weak (bifurcated) hydrogen bond between NH(P) of one molecule and CO(P) of another should lower this frequency somewhat. It therefore seems reasonable to associate the 3314 MS cm^{-1} band with NH(G) and the 3240 S, b cm^{-1} band with an overlap of NH(L) and NH(P). (The higher calculated frequency for Gly results

TABLE 1

Additional force constants for Pro-Leu-Gly-NH_2

	Force Constant[a]	Value[b]	Force Constant	Value
Prolyl ring:	f(NH)	5.674		
	$f(C^{\alpha}NH)$	0.650		
	$f(C^{\delta}NH)$	0.650		
	f(N . . . H)	0.050		
	f(HN . . . H ib)	0.010		
	$f(C^{\alpha}N$ . . . H ib)	0.050		
	$f(C^{\delta}N$ . . . H ib)	0.050		
$CONH_2$ group:	f(CO)	8.430	f(NH,NH)	−0.120
	f(CN)	6.450	f(CO,NCO)	0.520
	f(NH)	6.000	$f(CO,C^{\alpha}CO)$	0.190
	f(O . . . H)	0.100	$f(CO,C^{\alpha}CN)$[d]	−0.150
	$f(C^{\alpha}CO)$	1.250	$f(C^{\alpha}C,C^{\alpha}CN)$	0.080
	$f(C^{\alpha}CN)$	1.280	$f(C^{\alpha}C,C^{\alpha}CO)$	0.170
	f(NCO)	2.500	$f(CN,C^{\alpha}CN)$	−0.080
	f(CNH)	0.590	f(CN,NCO)	0.670
	f(HNH)	0.320	f(CN,CNH)	0.180
	f(NH . . . O ib,I)[c]	0.040	f(NH,CNH)	0.150
	f(NH . . . O ib,X)[c]	0.056	f(NH,HNH)	−0.080
	f(CO ob)	0.382	f(NCO,CNH)[d]	0.251
	$f(NH_2$ t)	0.500	f(CO ob,NH_2 t)	−0.016
	$f(NH_2$ w)	0.140	f(CO ob,NH_2 w)	0.023
	f(CO,CN)	0.370	f(NH_2 t,NH_2 w)	−0.106
	f(CN,NH)	0.280		

[a] f(AB) = AB bond stretch, f(ABC) = ABC angle bend, f(X,Y) = XY interaction; ib = in-plane angle bend, ob = out-of-plane angle bend, t = torsion, w = wag.

[b] Units are mdyn/A for stretch and stretch, stretch force constants, mdyn for stretch, bend force constants, and mdyn · A for all others.

[c] I = internal hydrogen bond, X = external hydrogen bond.

[d] From poly (glycine I) force field, ref. 21.

from the higher f(NH) force constant in poly (glycine I) (21) as compared to that in β-poly (L-alanine) (22), which was used for Leu and Pro.) It is interesting that the small shifts in amide A modes on temperature change are mirrored in the amide B modes: 3005 M and ~3060 sh cm^{-1} at room temperature and 3032 M and 3060 W cm^{-1} at low temperature. It may be that cell contraction changes the molecular conformation slightly, altering the internal HNH . . . O = C hydrogen bond, but has relatively little effect on the hydrogen bonds formed by the peptide groups.

On *N*-deuteration a complex pattern of bands related to ND stretch is found in the region of 2300–2600 cm^{-1}. Keeping in mind that more complex (possibly three-level) Fermi resonances can occur in this region (30), and that calculated frequencies are of the order of 50 cm^{-1} below observed values (30), a reasonable assignment of bands nevertheless seems possible. The ND_2 antisymmetric and symmetric stretch modes can be satisfactorily assigned to i.r. bands at 2552 S and 2403 MS cm^{-1}, respectively. (Analogous bands, not shown in the Figures, are seen in the Raman spectra.) It is interesting that these bands hardly shift at low temperature (2552 VS and 2405 S cm^{-1}, respectively), indicating perhaps that very little conformational change in the molecule occurs on cooling. Other bands are assignable to ND stretch, although the exact association must be considered tentative at this stage since a Fermi resonance analysis has not been done. They do

TABLE 2

Observed and calculated frequencies (cm^{-1}) of Pro-Leu-Gly-NH_2

Observed[a]		Calc.	Potential energy distribution[b]
Raman	i.r.		
3389 VW	3395 VS	3395	NH_2 as(99)
	3314 MS	3285[c]	NH(G) s(98)
		3239	NH_2 ss(97)
3235 W,b	3240 S,b	3238[c]	NH(L) s(98)
		3237[c]	NH(P) s(98)
	3060 sh		amide B
	3035 M		
		2984	$CH_3(\delta_2)$ as2(26), $CH_3(\delta_1)$ as2(25), $CH_3(\delta_2)$ as1(24), $CH_3(\delta_1)$ as1(24)
		2983	$CH_3(\delta_2)$ as1(27), $CH_3(\delta_2)$ as2(25),
2979 MS	2976 sh		$CH_3(\delta_1)$ as1(24), $CH_3(\delta_1)$ as2(23)
		2983	$CH_3(\delta_1)$ as2(48), $CH_3(\delta_2)$ as2(43)
		2982	$CH_3(\delta_1)$ as1(47), $CH_3(\delta_2)$ as1(44)
2971 MS	2966 S	2965	$CH_2(P\gamma)$ as(48), $CH_2(P\beta)$ as(35), $CH_2(P\delta)$ as(17)
2963 M	2960 sh	2960	$CH_2(P\delta)$ as(55), $CH_2(P\beta)$ as(43)
	2946 S	2957	$CH_2(P\gamma)$ as(50), $CH_2(P\delta)$ as(28), $CH_2(P\beta)$ as(22)
		2930	$CH_3(\delta_1)$ ss(50), $CH_3(\delta_2)$ ss(47)
2938 VS	2935 sh	2930	$CH_3(\delta_2)$ ss(52), $CH_3(\delta_1)$ ss(48)
		2928	CH_2(G) as(99)
2926 sh	2926 VW	2923	$CH_2(L\beta)$ as(87), $C^{\gamma}H$(L) s(10)
		2914	$C^{\gamma}H$(L) s(86), $CH_2(L\beta)$ as(11)
		2904	$C^{\alpha}H^{\alpha}$(P) s(65), $CH_2(P\delta)$ ss(15), $CH_2(P\gamma)$ ss(12), $CH_2(P\beta)$ ss(7)
		2903	$C^{\alpha}H^{\alpha}$(P) s(33), $CH_2(P\delta)$ ss(30), $CH_2(P\beta)$ ss(19), $CH_2(P\gamma)$ ss(16)
2899 MW	2900 sh	2901	$CH_2(P\delta)$ ss(53), $CH_2(P\beta)$ ss(28), $CH_2(P\gamma)$ ss(18)
		2900	$CH_2(P\gamma)$ ss(53), $CH_2(P\beta)$ ss(45)
2875 S	2872 MS	2866	$C^{\alpha}H$(L) s(94)
		2860	CH_2(G) ss(99)
2857 W	2855 sh	2855	$CH_2(L\beta)$ ss(94)
1691 MW	1680 VS	1680	CO(P) s(39), CO(L) s(33), CN(PL) s(11), CN(LG) s(9)
1664 sh	1662 M	1664	CO(L) s(41), CO(P) s(32), CN(LG) s(11), CN(PL) s(8)
1652 S	1650 sh	1658	CO(G) s(55), C^{α}CN(G) d(15), $C^{\alpha}C$(G) s(9), NH_2 r(9), NH_2 b(6)
1615 MW	1615 MW	1617	NH_2 b(49), CN(T) s(32), CO(G) ib(10), CO(G) s(7)
	1565 sh	1568	NH(L) ib(31), $C^{\alpha}C$(P) s(16), CN(PL) s(10), CO(P) ib(9), NC^{α}(P) s(8), H^{α}(P) b2(7), CO(P) s(7), C^{α}NH(P) d(5)

TABLE 2 (continued)

Observed[a]		Calc.	Potential energy distribution[b]
Raman	i.r.		
	1556 VS	1545	NH(G) ib(46), CN(LG) s(21), $C^{\alpha}C$(L) s(13), CO(L) ib(11), NC^{α}(G) s(6)
		1498	NH(L) ib(23), $C^{\alpha}NH$(P) d(14), NC^{α}(P) s(13), $C^{\delta}NH$(P) d(13), CN(PL) s(10), CH_2(Pδ) b(6), $C^{\delta}N$(P) s(6)
1482 W		1479	CH_2(Pβ) b(79), CH_2(Pγ) b(10), CH_2(Pβ) w(6)
1467 M	1469 MW	1477	CH_2(Pδ) b(73), CH_2(Pδ) w(12)
		1458	$CH_3(\delta_1)$ ab1(35), $CH_3(\delta_2)$ ab1(24), $CH_3(\delta_1)$ ab2(11), $CH_3(\delta_1)$ r2(8), H^{γ}(L) b1(5), $CH_3(\delta_2)$ ab2(5)
		1454	CH_2(Pγ) b(74), CH_2(Pβ) b(11), $C^{\gamma}C^{\delta}$(P) s(6), CH_2(Pδ) w(6),
1451 VS	1456 VW		CH_2(Pγ) w(5)
		1453	CH_2(G) b(86), NH_2 b(6)
		1451	$CH_3(\delta_1)$ ab2(50), $CH_3(\delta_2)$ ab1(22), $CH_3(\delta_2)$ ab2(13), $CH_3(\delta_1)$ r1(6)
		1451	$CH_3(\delta_2)$ ab2(51), $CH_3(\delta_1)$ ab1(18), $CH_3(\delta_2)$ ab1(11), $CH_3(\delta_2)$ r1(8)
	1437 MW	1447	$CH_3(\delta_2)$ ab1(27), $CH_3(\delta_1)$ ab1(26), $CH_3(\delta_1)$ ab2(20), $CH_3(\delta_2)$ ab2(18)
1423 MW	1424 sh	1423	$C^{\alpha}C^{\beta}$(P) s(19), CH_2(Pβ) w(18), CH_2(Pδ) w(17), H^{α}(P) b1(13), CH_2(Pδ) b(11), CH_2(Pγ) w(5)
		1406	NH_2 b(21), CH_2(G) w(19), $C^{\alpha}C$(G) s(12), CO(G) ib(10), CN(T) s(8), CH_2(G) b(7)
		1404	CH_2(Pγ) w(56), $C^{\gamma}C^{\delta}$(P) s(17), CH_2(Pγ) b(12), CH_2(Pδ) w(10), $C^{\beta}C^{\gamma}$(P) s(6)
		1402	$CH_3(\delta_2)$ sb(63), H^{γ}(L) b1(9), CH_2(Lβ) tw(5), CH_2(Lβ) b(5)
		1401	$CH_3(\delta_1)$ sb(81), $CH_3(\delta_2)$ sb(8)
1395 MW	1394 sh	1396	CH_2(Lβ) b(31), $CH_3(\delta_2)$ sb(26), $C^{\gamma}C^{\delta}$(L2) s(13), $CH_3(\delta_1)$ sb(9), CH_2(Lβ) tw(8)
		1391	CH_2(Pδ) w(26), CH_2(Pγ) w(15), CH_2(Pβ) w(14), CH_2(Pδ) b(10), $C^{\alpha}C^{\beta}$(P) s(9), $C^{\beta}C^{\gamma}$(P) s(8), $C^{\delta}N$(P) s(8)
1384 VW	1386 M	1383	CH_2(Lβ) w(29), CH_2(Lβ) b(25), H^{γ}(L) b1(14), $C^{\beta}C^{\gamma}$(L) s(11), $C^{\gamma}C^{\delta}$(L1) s(9), $C^{\alpha}C^{\beta}$(L) s(5), $CH_3(\delta_1)$ sb(5)
1375 W	1370 M	1375	CH_2(Lβ) b(20), CH_2(Lβ) tw(19), CH_2(Lβ) w(12), H^{α}(L) b2(8), $C^{\gamma}C^{\delta}$(L2) s(6), H^{γ}(L) b1(5), NH(L) ib(5)

TABLE 2 (continued)

Observed[a]		Calc.	Potential energy distribution[b]
Raman	i.r.		
1351 MW		1354	CH_2(G) w(24), CH_2(Lβ) b(9), CH_2(Lβ) w(7), NH(G) ib(7), H^{α}(L) b2(6), NH_2 b(6), CO(G) ib(6)
		1350	H^{α}(P) b1(34), CH_2(Pβ) w(28), C^{α}NH(P) d(8), C^{δ}NH(P) d(8)
1345 M		1335	H^{α}(L) b2(25), CH_2(G) w(16), C^{δ}NH(P) d(7), H^{α}(P) b2(7), NH(L) ib(6)
1338 M	1336 M	1328	CH_2(G) w(20), H^{α}(P) b2(10), NH(L) ib(9), C^{δ}NH(P) d(8), H^{α}(L) b2(6)
1310 MW	1314 W	1300	CH_2(Lβ) tw(27), CH_2(Lβ) w(18), H^{γ}(L) b1(13), H^{α}(L) b1(8), $C^{\beta}C^{\gamma}$(L) s(6), NC^{α}(L) s(5)
1288 MW	1285 MW	1282	H^{γ}(L) b2(37), CH_2(Lβ) w(18), H^{α}(L) b2(9), $C^{\gamma}C^{\delta}$(L1) s(9), H^{α}(L) b1(6), $C^{\gamma}C^{\delta}$(L2) s(5)
1271 MS	1270 sh	1266	H^{α}(P) b2(16), H^{α}(L) b2(10), NH(G) ib(9), CN(PL) s(7), CH_2(G) w(6), NC^{α}(L) s(5)
1263 W	1261 M	1244	CH_2(G) tw(85), NH(G) ib(8)
1241 S	1241 M	1237	$C^{\beta}C^{\gamma}$(L) s(13), H^{α}(L) b2(9), NC^{α}(L) s(7), NC^{α}(G) s(6), NH(L) ib(5)
1223 MW	1219 MW	1220	$C^{\beta}C^{\gamma}$(L) s(14), H^{α}(L) b1(9), NC^{α}(G) s(6), H^{α}(L) b2(6), H^{γ}(L) b1(6), CN(LG) s(5)
1189 W	1187 W	1196	H^{γ}(L) b2(28), $C^{\gamma}C^{\delta}$(L2) s(12), H^{α}(L) b1(8), H^{γ}(L) b1(7)
1177 MW	1174 sh	1168	$C^{\alpha}C^{\beta}$(L) s(27), NC^{α}(L) s(12), H^{γ}(L) b1(9), $C^{\gamma}C^{\delta}$(L1) s(6), $CH_3(\delta_1)$ r1(6)
	1165 MW	1164	H^{α}(P) b1(21), NC^{α}(P) s(13), CH_2(Pγ) tw(11), $C^{\alpha}C^{\beta}$(P) s(9)
		1154	CH_2(Pγ) tw(41), CH_2(Pβ) tw(13), CH_2(Pδ) tw(12)
		1144	H^{α}(L) b1(27), NC^{α}(G) s(13), $C^{\gamma}C^{\delta}$(L1) s(9), NC^{α}(L) s(6)
1135 S	1130 W	1134	NH_2 r(59), CO(G) s(16), CN(T) s(6), C^{α}C(G) s(6)
		1125	$C^{\alpha}C^{\beta}$(L) s(38), NC^{α}(G) s(11), $C^{\gamma}C^{\delta}$(L1) s(9), $CH_3(\delta_2)$ r1(8), $CH_3(\delta_1)$ r1(6)
	1118 MW	1115	CH_2(Pβ) tw(22), CH_2(Pδ) w(10), CH_2(Pδ) tw(9), C^{δ}N(P) s(8), $C^{\beta}C^{\gamma}$(P) s(7), CH_2(Pβ) w(5)
1103 M	1104 W	1109	CH_2 (Pδ) tw(35), CH_2 (Pβ) tw(18), $C^{\gamma}C^{\delta}$(P) s(6), C^{δ}N(P) s(6), CH_2(Pδ) w(5)

TABLE 2 (continued)

Observed[a]		Calc.	Potential energy distribution[b]
Raman	i.r.		
1089 MW	1087 MW	1079	NC^{α}(G) s(28), H^{α}(L) b1(18), CH_2(Lβ) tw(13), $CH_3(\delta_1)$ r1(10)
1050 W	1046 sh	1048	CH_2(G) tw(24), CH_2(Pβ) tw(22), CH_2(Pδ) tw(20), H^{α}(P) b2(7)
1041 M	1038 W	1032	NC^{α}(G) s(16), NC^{α}(L) s(14), $CH_3(\delta_1)$ r1(12), CH_2(G) r(9), CN(LG) s(8), $C^{\alpha}C^{\beta}$(L) s(7)
1013 MS	1009 W	1012	$CH_3(\delta_2)$ r2(47), $CH_3(\delta_1)$ r1(23), $CH_3(\delta_1)$ r2(7)
		995	CH_2(G) r(42), CNC^{α}(L) d(6)
988 W	984 MW	988	$CH_3(\delta_1)$ r2(48), $CH_3(\delta_2)$ r1(11), $C^{\gamma}C^{\delta}$(L2) s(8), $CH_3(\delta_1)$ r1(7), $C^{\beta}C^{\gamma}$(L) s(5)
976 W	976 W	982	$C^{\beta}C^{\gamma}$(P) s(18), $C^{\alpha}C^{\beta}$(P) s(10), CH_2(Pδ) r(10), CH_2(G) r(7), C^{δ}NH(P) d(7), CH_2(Pβ) r(6)
		979	$CH_3(\delta_2)$ r1(43), $C^{\gamma}C^{\delta}$(L1) s(17), $C^{\beta}C^{\gamma}$(L) s(11)
962 MS	958 VW	974	NC^{α}(P) s(9), CH_2(Pδ) tw(9), C^{α}C(P) s(7), C^{δ}N(P) s(7), $C^{\alpha}C^{\beta}$(P) s(5), H^{α}(P) b2(5), CN(PL) s(5)
957 M		963	C^{δ}N(P) s(18), $C^{\beta}C^{\gamma}$(P) s(12), CH_2(Pβ) r(11), CH_2(Pγ) r(9), $C^{\gamma}C^{\delta}$(P) s(7), H^{α}(P) b1(7)
921 VS	920 M	921	C^{α}NH(P) d(22), $C^{\gamma}C^{\delta}$(P) s(15), CH_2(Pγ) tw(9), CH_2(Pβ) tw(6), C^{δ}NH(P) d(6), CH_2(Pδ) tw(6)
916 VS	914 M	908	$C^{\gamma}C^{\delta}$(L2) s(17), C^{α}C(L) s(16), CH_2(G) r(9), CH_2(Lβ) r(8), NC^{α}C(L) d(7)
	890 VW	892	CH_2(Lβ) r(14), NC^{α}(L) s(11), $C^{\beta}C^{\gamma}$(L) s(10), $C^{\gamma}C^{\delta}$(P) s(10), $CH_3(\delta_1)$ r1(7), $C^{\beta}C^{\gamma}$(P) s(6), $CH_3(\delta_2)$ r2(6)
876 VS		885	$C^{\gamma}C^{\delta}$(P) s(16), $C^{\beta}C^{\gamma}$(P) s(9), CN(PL) s(7), C^{δ}NH(P) d(7)
	868 W	877	CN(T) t(28), CN(T) s(12), NH_2 w(12), CO(G) s(6), CO(G) ib(5)
		859	CN(T) s(19), CN(T) t(19), CO(G) s(9), CO(G) ib(7), C^{α}C(G) s(7)
	851 VW	853	$C^{\alpha}C^{\beta}$(P) s(12), C^{α}C(P) s(9), $C^{\beta}C^{\gamma}$(P) s(9), NC^{α}(P) s(6), CH_2(Pδ) r(5), CO(P) ib(5)
836 W		843	CH_2(Lβ) r(16), $C^{\gamma}C^{\delta}$(L2) s(11), CH_2(G) r(11), C^{α}C(L) s(10), CN(LG) s(7), CN(T) t(6), $C^{\gamma}C^{\delta}$(L1) s(5)

TABLE 2 (continued)

Observed[a]		Calc.	Potential energy distribution[b]
Raman	i.r.		
777 W	783 W	802	$CH_2(P\delta)$ r(26), $CH_2(P\beta)$ r(15), $C^{\alpha}NH(P)$ d(9), $C^{\alpha}C^{\beta}(P)$ s(7), $NC^{\alpha}C(P)$ d(5)
		751	CO(P) ob(17), CO(L) ib(10), NH_2 w(9)
749 MW	747 MS	739	NH_2 w(23), CO(P) ob(16), NH . . . O(TX) d(12), CN(T) t(9), CN(LG) t(7), $C^{\alpha}C(G)$ s(6)
		722	NH_2 w(22), NH . . . O(TX) d(5), CN(PL) t(12), CO(L) ib(10), CN(T) t(8)
		704	CN(LG) t(23), CO(G) ib(9), NH_2 w(8), CO(L) ib(7), $C^{\alpha}C(G)$ s(7), CO(L) ob(5), NH . . . O(TX) d(5), NH . . . O(G) d(5)
695 W,b	687 MS	699	CN(PL) t(46), NH(L) ob(24), NH . . . O(L) d(16)
		689	$CH_2(P\beta)$ r(21), CO(P) ib(11), $C^{\alpha}C(P)$ s(9), $C^{\gamma}C^{\delta}N(P)$ d(9), $C^{\beta}C^{\gamma}C^{\delta}(P)$ d(8), CN(PL) t(8), $NC^{\alpha}C(P)$ d(6), $C^{\alpha}NC^{\delta}(P)$ d(6)
	664 VW	669	CO(P) ib(10), $CH_2(P\gamma)$ r(9), $C^{\alpha}C(P)$ s(9), $C^{\alpha}C^{\beta}(P)$ s(8), CO(P) ob(8), $C^{\alpha}NC^{\delta}(P)$ d(6), CN(PL) t(6), $C^{\beta}(P)$ b2(5)
647 W	645 S	657	$C^{\alpha}C^{\beta}C^{\gamma}(P)$ d(15), CO(P) ob(11), $C^{\beta}(P)$ b2(10), $CH_2(P\gamma)$ r(9), $CH_2(P\delta)$ r(9), $C^{\beta}C^{\gamma}C^{\delta}(P)$ d(8), $C^{\alpha}NC^{\delta}(P)$ d(7), $NC^{\alpha}C(P)$ d(6), NH(L) ob(6)
		632	CO(L) ob(59), $C^{\alpha}C(G)$ s(12), $C^{\beta}(L)$ b1(7), CO(G) ib(6)
614 W	612 MS	603	CN(LG) t(40), NH(G) ob(30), NH . . . O(G) d(18), CO(L) ob(14), $C^{\alpha}C(G)$ s(10), CO(G) ib(9), $C^{\alpha}CN(L)$ d(7), $CH_2(G)$ w(5)
571 M	570 MS	575	CN(LG) t(18), $C^{\alpha}CN(G)$ d(16), NH(G) ob(15), $NC^{\alpha}C(G)$ d(10), $C^{\alpha}CN(L)$ d(10), $NC^{\alpha}C(L)$ d(8), NH . . . O(G) d(8)
542 W	537 MW	566	$CH_2(P\gamma)$ r(31), $CH_2(P\beta)$ r(16), $CH_2(P\delta)$ r(15), $C^{\beta}C^{\gamma}C^{\delta}(P)$ d(13), $C^{\gamma}C^{\delta}N(P)$ d(12), $C^{\alpha}C^{\beta}C^{\gamma}(P)$ d(5)
500 M		502	$C^{\alpha}CN(G)$ d(24), CO(G) ib(15), $C^{\alpha}C^{\beta}C^{\gamma}(L)$ d(7), $C^{\beta}(L)$ b2(6), $NC^{\alpha}(G)$ s(6), $NC^{\alpha}C(L)$ d(5), $NC^{\alpha}C(G)$ d(5)
		473	O . . . H(L) s(93)
453 W		449	CO(G) ob(74), $C^{\gamma}(L)$ sd(8)

TABLE 2 (continued)

Observed[a]		Calc.	Potential energy distribution[b]
Raman	i.r.;		
425 W		441	C^{γ}(L) sd(23), CO(G) ob(21), O . . . H(PX) s(14)
		433	O . . . H(PX) s(80)
404 MW		410	O . . . H(G) s(90)
		392	C^{γ}(L) sd(35), C^{γ}(P) b2(12), C^{γ}(P) b1(11), $C^{\alpha}C^{\beta}C^{\gamma}$(L) d(7), CO(L) ib(6)
		380	C^{γ}(P) b2(42), C^{γ}(P) b1(14), C^{β}(L) b1(7)
354 W		342	C^{γ}(P) b1(13), C^{β}(P) b2(11), CO(L) ib(9), C^{α}CN(L) d(8), NH(L) ob(8), CNC^{α}(L) d(7)
332 MW		332	N . . . H(P) s(30), C^{β}(P) b1(18), CO(P) ib(12), NC^{α}C(P) d(8), NH . . . O(P) d(5)
318 MW		310	NC^{α}C(G) d(17), CNC^{α}(L) d(14), C^{α}CN(G) d(10), C^{β}(L) b2(9), C^{β}(P) b2(6)
295 S		283	C^{γ}(P) b1(20), NC^{α}C(G) d(11), N . . . H(P) s(10), NH(G) ob(7), $C^{\gamma}C^{\delta}$(L2) t(7), C^{β}(L) b1(6), $C^{\gamma}C^{\delta}$(L1) t(5), CO(P) ib(5)
280 W		281	N . . . H(P) s(47), NC^{α}C(P) d(6), C^{β}(L) b1(6), C^{β}(L) b2(5)
		269	N . . . H(P) s(10), NC^{α}C(L) d(9), NC^{α}C(G) d(9), C^{β}(P) b1(8), CO(L) ib(7), CO(P) ob(7), C^{γ}(P) b2(6)
		260	C^{α}CN(P) d(19), C^{β}(L) b1(14), CNC^{α}(L) d(13), NH(G) ob(10), NC^{α}C(G) d(7), NC^{α}(L) s(7)
		245	$C^{\gamma}C^{\delta}$(L1) t(60), $C^{\gamma}C^{\delta}$(L2) t(38)
		236	$C^{\gamma}C^{\delta}$(L2) t(42), $C^{\gamma}C^{\delta}$(L1) t(27)
		224	C^{α}CN(L) d(24), CNC^{α}(L) d(11), C^{γ}(P) b1(10), C^{α}CN(P) d(7)
		208	NC^{α}C(G) d(16), $C^{\alpha}C^{\beta}C^{\gamma}$(L) d(9), C^{γ}(P) b2(9), NH(G) ob(9), CNC^{α}(P) d(8)
		201	C^{δ}N . . . H(P) d(32), C^{α}N . . . H(P) d(26)
		188	C^{α}N . . . H(P) d(19), $C^{\gamma}C^{\delta}$(P) t(10), C^{δ}N . . . H(P) d(8), $C^{\beta}C^{\gamma}$(P) t(7), $C^{\gamma}C^{\delta}$N(P) d(6), $C^{\beta}C^{\gamma}C^{\delta}$(P) d(6)
		164	C^{α}N . . . H(P) d(27), C^{δ}N . . . H(P) d(24), HN . . . H(P) d(17), NC^{α}(P) t(9), NC^{δ}(P) t(9)
		148	CO(G) t(21), H . . . O(L) s(11), CNC^{α}(P) d(8), H . . . O(T) s(8)
		135	CO(G) t(60), H . . . O(G) s(9)
		133	CO(L) t(71), H . . . O(G) s(12)

TABLE 2 (continued)

Observed[a]		Calc.	Potential energy distribution[b]
Raman	i.r.		
		128	H . . . O(P) s(26), H . . . O(G) s(20), H . . . O(T) s(12), CO(L) t(8)
		126	H . . . O(P) s(54), H . . . O(G) s(15), H . . . O(T) s(12), CO(G) t(6)
		123	H . . . O(G) s(31), H . . . O(T) s(14), H . . . O(L) s(7), CO(G) t(7)
		117	H . . . O(T) s(13), O . . . H(PI) s(13), O . . . H(L) s(13), C^{β}(L) b2(9), NH(L) ob(8), $C^{\alpha}C^{\beta}C^{\gamma}$(L) d(7), H . . . O(P) s(6)
		113	H . . . O(L) s(46), CNC^{α}(P) d(9), $C^{\alpha}C^{\beta}$(P) t(6)
		98	O . . . H(PI) s(30), H . . . O(T) s(14) NH . . . O(P) d(7)
		85	CO . . . H(L) d(18), $C^{\alpha}C^{\beta}$(P) t(6), NH(G) ob(5)
		83	CO . . . H(G) d(68), CO . . . H(L) d(7)
		79	CO . . . H(L) d(34), $C^{\alpha}C^{\beta}C^{\gamma}$(L) d(8), CO . . . H(G) d(7), $NC^{\alpha}C$(L) d(6), NH . . . O(TX) d(5), NH(L) ob (5)
		73	NH(G) ob(16), NH . . . O(L) d(12), NH(TX) t(10), CN(PL) t(7)
		64	NH . . . O(TX) d(31), NH_2 w(24), CN(T) t(17), CO . . . H(L) d(12), NH(G) ob(6)
		59	CO . . . H(L) d(12), NH . . . O(P) d(11), NH(TX) t(9), NH(L) ob(8), C^{β}(L) b1(6), CO . . . H(G) d(6), $C^{\alpha}C$(G) t(6), $NC^{\alpha}C$(L) d(6)
		51	CO . . . H(PX) d(53), CN(LG) t(9), NH . . . O(G) d(7), NH(G) ob(6)
		51	CO . . . H(PX) d(43), CN(LG) t(12), NH . . . O(G) d(10), NH(G) ob(7), $C^{\beta}C^{\gamma}$(L) t(6)
		45	$C^{\beta}C^{\gamma}$(L) t(27), NH(TX) t(8), $C^{\alpha}C$(P) t(7), $C^{\alpha}C$(G) t(6)
		43	NH . . . O(P) d(19), $C^{\beta}C^{\gamma}$(L) t(11), $C^{\alpha}C$(G) t(7), $C^{\alpha}C$(P) t(6), NH . . . O(L) d(6), $C^{\alpha}C^{\beta}$(L) t(5), CNC^{α}(P) d(5)
		35	$C^{\alpha}C^{\beta}$(L) t(40), $C^{\beta}C^{\gamma}$(L) t(18), CO(P) t(10), NH(TX) t(5)
		34	CO(P) t(81)
		30	NH . . . O(L) d(18), NH . . . O(P) d(10), O . . . H(PI) s(7), CN(PL) t(7), $C^{\beta}C^{\gamma}$(L) t(6), $NC^{\alpha}C$(L) d(5)
		28	NH(TX) t(33), $C^{\alpha}C$(G) t(17), NH(L) ob(10), NH . . . O(L) d(6)
		25	NH(G) t(36), $C^{\alpha}C^{\beta}$(L) t(15), NH(L) ob(7), NH(L) t(7),

TABLE 2 (continued)

Observed[a]		Calc.	Potential energy distribution[b]
Raman	i.r.		
			NH . . . O(G) d(6), NH . . . O(L) d(5)
		24	NH(L) t(78), $C^{\alpha}C^{\beta}$(L) t(10)
		22	NH(G) t(29), NH(L) ob(17), C^{α}C(P) t(9), NC^{α}(L) t(9), NH(TX) t(8), NH . . . O(L) d(7), C^{β}(L) bl(6)
		21	NC^{α}(G) t(34), C^{α}C(L) t(15), NH . . . O(G) d(15), NH(G) t(8), NH(G) ob(7)
		16	C^{α}C(P) t(38), NH . . . O(P) d(9), NC^{α}(G) t(8), O . . . H(PI) s(7)
		11	C^{α}C(L) t(16), NH(P) t(11), NC^{α}(G) t(11), C^{α}C(P) t(10), CO . . . H(PI) d(10), NH(TI) t(9), NH . . . O(TI) d(8), NH(G) ob(8), NC^{α}(L) t(7)
		8	NH(P) t(84), C^{α}C(P) t(9)

[a] S = strong, M = medium, W = weak, V = very, sh = shoulder, b = broad.
[b] s = stretch, as = antisymmetric stretch, ss = symmetric stretch, b = angle bend, ib = in-plane angle bend, ob = out-of-plane angle bend, w = wag, r = rock, t = torsion, d = deformation, sd = symmetric deformation, tw = twist, L = leucine, G = glycine, P = proline, T = terminal. Numbers 1 and 2 following L refer to $C^{\delta}1$ and $C^{\delta}2$ of leucine respectively. X refers to external and I refers to intra. In O . . . H and H . . . O the first atom belongs to the residue in the bracket and the second atom is either an intramolecular or an externally added atom. In the case of NH . . . O and CO . . . H the groups NH or CO belong to the residue in the bracket. Only contributions of 5% or greater are included.
[c] Unperturbed frequency.

not shift in frequency on cooling, but there are some changes in relative intensities.

The region of the CH stretch modes is complex, since CH_3, CH_2, and CH groups are present. It is nevertheless interesting that all of the observed bands are well accounted for by the calculations.

The amide I region contains bands that are mostly CO stretch, mixed with each other and with NH_2 modes. The 1680 VS cm^{-1} band in the i.r. is well assigned to mixed CO(P) and CO(L) stretch (the Raman counterpart, at 1691 cm^{-1} is not coincident, perhaps as a result of intermolecular effects); its 5 cm^{-1} downward shift on *N*-deuteration is well reproduced. Another such mode is found near 1660 cm^{-1}. Because of the smaller f(CO) constant in the $CONH_2$ group (8.430 vs. 9.882 mdyn/Å in Pro and Leu), CO(G) stretch is expected to be the lowest such frequency; it is well predicted as corresponding to the 1652 S cm^{-1} Raman band. This mode contains only CO(G) stretch, but it also has an admixture of small contributions from NH_2 rock and bend. (The main NH_2 bend mode, with a small contribution from CO(G) stretch, occurs at 1615 cm^{-1}.) This accounts for its large predicted (18 cm^{-1}), and observed (17 cm^{-1}), downward shift on *N*-deuteration. Similar shifts on *N*-deuteration have been observed for acetamide (25, 26). It is therefore unnecessary to invoke a conformational change in the molecule as the source of this shift (11).

The amide II region exhibits only one strong band in the i.r., at 1556 cm^{-1}, which is moderately well predicted by the calculation. (A very weak and broad band at ~1510 cm^{-1} in the low temperature spectrum may correspond to the predicted mode at 1498 cm^{-1}.) This contrasts with the multiple bands seen for a type I

TABLE 3

Observed and calculated frequencies (cm^{-1}) of N-*deuterated Pro-Leu-Gly-*NH_2

Observed[a]		Calc.	Potential energy distribution[b]
Raman	i.r.		
		2984	$CH_3(\delta_2)$ as2(27), $CH_3(\delta_1)$ as2(24), $CH_3(\delta_1)$ as1(24), $CH_3(\delta_2)$ as1(23)
2980 S	2975 sh	2983	$CH_3(\delta_2)$ as1(28), $CH_3(\delta_2)$ as2(26), $CH_3(\delta_1)$ as1(24), $CH_3(\delta_1)$ as2(21)
		2983	$CH_3(\delta_1)$ as2(50), $CH_3(\delta_2)$ as2(41)
		2982	$CH_3(\delta_1)$ as1(47), $CH_3(\delta_2)$ as1(44)
2971 S	2968 S	2965	$CH_2(P\gamma)$ as(47), $CH_2(P\beta)$ as(35), $CH_2(P\delta)$ as(17)
2962 M	2960 S	2960	$CH_2(P\delta)$ as(56), $CH_2(P\beta)$ as(42)
	2948 S	2956	$CH_2(P\gamma)$ as(51), $CH_2(P\delta)$ as(27), $CH_2(P\beta)$ as(22)
2936 sh	2939 VS	2930	$CH_3(\delta_1)$ ss(51), $CH_3(\delta_2)$ ss(46)
		2930	$CH_3(\delta_2)$ ss(53), $CH_3(\delta_1)$ ss(47)
2922 M		2928	CH_2(G) as(99)
		2923	$CH_2(L\beta)$ as(87), $C^{\gamma}H$(L) s(10)
		2913	$C^{\gamma}H$(L) s(86), $CH_2(L\beta)$ as(11)
		2904	$C^{\alpha}H^{\alpha}$(P) s(63), $CH_2(P\delta)$ ss(16), $CH_2(P\gamma)$ ss(13), $CH_2(P\beta)$ ss(7)
		2903	$C^{\alpha}H^{\alpha}$(P) s(35), $CH_2(P\delta)$ ss(29), $CH_2(P\beta)$ ss(18), $CH_2(P\gamma)$ ss(17)
2901 M	2905 sh	2901	$CH_2(P\delta)$ ss(52), $CH_2(P\beta)$ ss(34), $CH_2(P\gamma)$ ss(13)
		2900	$CH_2(P\gamma)$ ss(57), $CH_2(P\beta)$ ss(40)
2875 S	2872 S	2866	$C^{\alpha}H$(L) s(94)
		2860	CH_2(G) ss(99)
2856 sh	2855 sh	2855	$CH_2(L\beta)$ ss(94)
2550 MW	2552 S	2518	ND_2 as(99)
2494 VW	2492 W		
2465 W	2464 W	2412	ND(G) s(96)
		2377	ND(L) s(96)
		2374	ND(P) s(96)
2402 MW	2403 MS	2343	ND_2 ss(95)
2340 W,b	2328 W		
1676 M	1675 VS	1675	CO(L) s(44), CO(P) s(28), CN(LG) s(13), CN(PL) s(8)
1659 sh	1652 S	1660	CO(P) s(44), CO(L) s(30), CN(PL) s(12), CN(LG) s(8), C^{α}CN(P) d(5)
1635 S	1640 sh	1640	CO(G) s(66), C^{α}CN(G) d(16), CN(T) s(15), $C^{\alpha}C$(G) s(5)
	1520 VW	1513	$C^{\alpha}C$(P) s(25), H^{α}(P) b2(15), NC^{α}(P) s(13), CO(P) s(13), CO(P) ib(11), CN(PL) s(8), $CH_2(P\beta)$ w(5)
1509 VW	1510 VW	1509	CN(T) s(34), CO(G) ib(27), $C^{\alpha}C$(G) s(26), CH_2(G) b(8), ND_2 b(5)
	1457 S	1484	CN(LG) s(26), $C^{\alpha}C$(L) s(25),

TABLE 3 (continued)

Observed[a]		Calc.	Potential energy distribution[b]
Raman	i.r.		
			CO(L) ib(17), CO(L) s(11), ND(G) ib(10), NC^{α}(G) s(6), H^{α}(L) b2(5)
		1479	$CH_2(P\beta)$ b(69), $CH_2(P\gamma)$ b(12), $CH_2(P\delta)$ b(9), $CH_2(P\beta)$ w(8)
1466 M	1468 W	1477	$CH_2(P\delta)$ b(71), $CH_2(P\delta)$ w(12), $CH_2(P\beta)$ b(8), $C^{\delta}N$(P) s(6)
		1458	$CH_3(\delta_1)$ ab1(34), $CH_3(\delta_2)$ ab1(24), $CH_3(\delta_1)$ ab2(11), $CH_3(\delta_1)$ r2(8), $CH_3(\delta_2)$ ab2(6)
		1454	$CH_2(P\gamma)$ b(72), $CH_2(P\beta)$ b(12), $C^{\gamma}C^{\delta}$(P) s(6), $CH_2(P\delta)$ w(6), $CH_2(P\gamma)$ w(5)
1451 S	1457 S	1451	$CH_3(\delta_1)$ ab2(51), $CH_2(\delta_2)$ ab1(23), $CH_3(\delta_2)$ ab2(10), $CH_3(\delta_1)$ r1(6)
		1451	$CH_3(\delta_2)$ ab2(53), $CH_3(\delta_1)$ ab1(19), $CH_3(\delta_2)$ ab1(10), $CH_3(\delta_2)$ r1(8)
	1437 VW	1447	$CH_3(\delta_2)$ ab1(27), $CH_3(\delta_1)$ ab1(26), $CH_3(\delta_1)$ ab2(20), $CH_3(\delta_2)$ ab2(18)
		1437	CH_2(G) b(87)
1423 VW	1427 M	1424	NC^{α}(P) s(23), H^{α}(P) b1(23), $C^{\alpha}C^{\beta}$(P) s(11), CN(PL) s(10), $CH_2(P\delta)$ w(5)
		1411	$CH_2(P\gamma)$ w(21), $CH_2(P\beta)$ w(20), $CH_2(P\delta)$ w(12), $CH_2(P\delta)$ b(10), CN(PL) s(9), $C^{\alpha}C^{\beta}$(P) s(5)
		1403	$CH_2(P\gamma)$ w(40), $C^{\gamma}C^{\delta}$(P) s(17), $CH_2(P\delta)$ w(17), $CH_2(P\gamma)$ b(11), $C^{\beta}C^{\gamma}$(P) s(6), $C^{\delta}N$(P) s(5)
		1402	$CH_3(\delta_2)$ sb(54), $CH_3(\delta_1)$ sb(37)
		1401	$CH_3(\delta_1)$ sb(52), $CH_3(\delta_2)$ sb(22), H^{γ}(L) b1(8)
1401 MW	1398 W	1395	$CH_2(L\beta)$ b(32), $CH_3(\delta_2)$ sb(18), $C^{\gamma}C^{\delta}$(L2) s(13), $CH_2(L\beta)$ tw(9), H^{γ}(L) b1(6)
		1385	$CH_2(P\beta)$ w(28), $CH_2(P\delta)$ w(15), $C^{\alpha}C^{\beta}$(P) s(13), $CH_2(P\gamma)$ w(13), $C^{\beta}C^{\gamma}$(P) s(12), $CH_2(P\beta)$ b(6)
1381 VW	1387 W	1383	$CH_2(L\beta)$ b(28), $CH_2(L\beta)$ w(23), H^{γ}(L) b1(20), $C^{\beta}C^{\gamma}$(L) s(12), $C^{\gamma}C^{\delta}$(L1) s(9)
	1370 MW	1369	$CH_2(L\beta)$ w(28), $CH_2(L\beta)$ b(26), $CH_2(L\beta)$ tw(18), $C^{\gamma}C^{\delta}$(L2) s(6), H^{γ}(L) b2(6)
1350 M	1345 sh	1342	CH_2(G) w(88)
1341 M	1334 MS	1316	H^{α}(L) b2(32), H^{γ}(L) b1(10), H^{α}(P) b1(9), $CH_2(P\beta)$ w(6), $CH_2(L\beta)$ w(6), $CH_2(L\beta)$ tw(6), NC^{α}(L) s(5)

TABLE 3 (continued)

Observed[a]		Calc.	Potential energy distribution[b]
Raman	i.r.		
1310 W		1311	H^{α}(P) b1(21), H^{α}(L) b2(17), $CH_2(P\beta)$ w(11), H^{α}(P) b2(7), H^{γ}(L) b2(5)
	1305 W	1293	$CH_2(L\beta)$ tw(23), H^{α}(L) b1(12), H^{γ}(L) b2(9), H^{α}(P) b1(7), $C^{\beta}C^{\gamma}$(L) s(6), $CH_2(L\beta)$ w(5)
1286 W	1286 W	1279	H^{γ}(L) b2(29), $CH_2(L\beta)$ w(26), H^{α}(L) b2(22), $C^{\gamma}C^{\delta}$(L1) s(7), H^{γ}(L) b1(6)
1263 MW	1261 W	1246	CH_2(G) tw(80), H^{α}(L) b2(6)
1252 M	1252 W	1228	H^{α}(P) b2(19), C^{δ}N(P) s(16), $C^{\beta}C^{\gamma}$(L) s(11), C^{δ}ND(P) d(7)
1223 W	1222 W	1224	$C^{\beta}C^{\gamma}$(L) s(16), H^{α}(P) b2(16), C^{δ}N(P) s(10), H^{γ}(L) b1(8), H^{α}(L) b1(5)
		1203	H^{γ}(L) b2(27), H^{α}(L) b1(18), H^{γ}(L) b1(8), $C^{\gamma}C^{\delta}$(L2) s(7), $CH_2(L\beta)$ tw(5)
1179 M	1175 W	1172	$C^{\alpha}C^{\beta}$(L) s(28), $C^{\gamma}C^{\delta}$(L1) s(10), NC^{α}(G) s(7), H^{α}(L) b1(7), $CH_2(L\beta)$ tw(6)
1168 sh	1164 W	1162	NC^{α}(L) s(17), $C^{\gamma}C^{\delta}$(L2) s(9), NC^{α}(G) s(8), $C^{\alpha}C^{\beta}$(L) s(6), H^{γ}(L) b1(6), $CH_3(\delta_1)$ r1(6), H^{α}(L) b1(5)
	1150 W	1158	$CH_2(P\gamma)$ tw(45), $CH_2(P\beta)$ tw(11), $CH_2(P\delta)$ tw(8), H^{α}(P) b1(6)
	1133 W	1133	$C^{\alpha}C^{\beta}$(L) s(18), $C^{\gamma}C^{\delta}$(L1) s(12), $CH_3(\delta_2)$ r1(8), H^{α}(L) b1(5)
1124 W	1124 W	1130	$C^{\alpha}C^{\beta}$(L) s(12), $C^{\alpha}C^{\beta}$(P) s(10), H^{α}(P) b1(7), $CH_2(P\beta)$ tw(7), $CH_2(P\beta)$ w(5), $C^{\gamma}C^{\delta}$(L1) s(5)
1100 W	1102 VW	1111	$CH_2(P\delta)$ tw(46), $CH_2(P\beta)$ tw(34), $CH_2(P\gamma)$ r(6)
1087 W		1097	ND_2 b(81), CO(G) ib(10), C^{α}C(G) s(8)
1083 W	1087 MW	1077	NC^{α}(G) s(29), H^{α}(L) b1(17), $CH_2(L\beta)$ tw(12), $CH_3(\delta_1)$ r1(10), C^{α}C(L) s(5)
1048 MW	1049 W	1051	$C^{\gamma}C^{\delta}$(P) s(16), $CH_2(P\beta)$ tw(13), $CH_2(P\gamma)$ tw(13), $CH_2(P\delta)$ tw(13), $C^{\beta}C^{\gamma}$(P) s(12), $CH_2(P\gamma)$ w(7), C^{δ}ND(P) d(6)
		1048	CH_2(G) r(29), ND(G) ib(21), NC^{α}(G) s(13), CNC^{α}(L) d(5)
1039 W	1038 W	1031	$C^{\gamma}C^{\delta}$(P) s(13), $CH_2(P\gamma)$ tw(12), $CH_2(P\beta)$ tw(9), C^{α}ND(P) d(8), C^{α}C(P) s(7), $C^{\alpha}C^{\beta}$(P) s(7), $CH_2(P\delta)$ tw(7)

TABLE 3 (continued)

Observed[a]		Calc.	Potential energy distribution[b]
Raman	i.r.		
1022 MW	1022 W	1019	$CH_3(\delta_1)$ r1(24), NC^{α}(G) s(9), NC^{α}(L) s(9), ND(G) ib(7)
	1005 VW	1011	$CH_3(\delta_2)$ r2(39), $CH_3(\delta_1)$ r2(10), $CH_3(\delta_1)$ r1(7), ND(L) ib(6)
		1002	ND(L) ib(28), $CH_3(\delta_1)$ r2(11), $CH_3(\delta_2)$ r2(8), $C^{\beta}C^{\gamma}$(L) s(6), $C^{\alpha}C$(P) s(6)
994 W	987 W	985	$CH_3(\delta_2)$ r1(36), $CH_3(\delta_1)$ r2(24), $CH_3(\delta_1)$ r1(8), $C^{\gamma}C^{\delta}$(L1) s(8) $C^{\gamma}C^{\delta}$(L2) s(7)
	979 VW	976	$CH_3(\delta_2)$ r1(20), $CH_3(\delta_1)$ r2(14), $C^{\beta}C^{\gamma}$(L) s(12), $C^{\gamma}C^{\delta}$(L1) s(9)
		971	$CH_2(P\beta)$ r(20), $CH_2(P\gamma)$ r(19), $CH_2(P\delta)$ r(18), $CH_2(P\delta)$ tw(8), $C^{\beta}C^{\gamma}$(P) s(5)
	968 VW	956	ND(L) ib(18), $C^{\delta}N$(P) s(12), $C^{\beta}C^{\gamma}$(P) s(10), NC^{α}(P) s(9), $CH_2(P\delta)$ tw(6)
957 MS			
	951 W	947	ND_2 r(31), CO(G) s(17), CN(T) s(11), ND(G) ib(7), CH_2(G) r(5)
	935 sh	932	ND(G) ib(35), CH_2(G) r(14), CN(LG) s(9), CO(L) s(7), ND_2 r(6)
	920 MW	917	$C^{\beta}C^{\gamma}$(P) s(27), CN(PL) s(8), $C^{\alpha}C$(P) s(8), $C^{\gamma}C^{\delta}$(P) s(8), $C^{\delta}ND$(P) d(8), CO(P) s(5), ND(L) ib(5)
917 VS	914 MW	903	$C^{\gamma}C^{\delta}$(L2) s(20), $C^{\alpha}C$(L) s(14), CH_2(G) r(13), $NC^{\alpha}C$(L) d(7), $C^{\alpha}C^{\beta}C^{\gamma}$(L) d(6)
886 VW	884 VW	885	$CH_2(L\beta)$ r(20), NC^{α}(L) s(13), $C^{\beta}C^{\gamma}$(L) s(12), $CH_3(\delta_1)$ r1(7), $CH_3(\delta_2)$ r2(7), $C^{\gamma}C^{\delta}$(L1) s(6), H^{α}(L) b1(5)
861 MS	859 W	854	$C^{\gamma}C^{\delta}$(P) s(22), $C^{\alpha}ND$(P) d(20), $C^{\delta}N$(P) s(9), $C^{\delta}ND$(P) d(7)
		851	$CH_2(P\delta)$ r(14), $C^{\alpha}C^{\beta}$(P) s(9), $C^{\beta}C^{\gamma}$(P) s(9), $C^{\alpha}C$(P) s(9), $NC^{\alpha}C$(P) d(7), $CH_2(P\beta)$ tw(6), $C^{\alpha}CN$(P) d(5)
836 W		841	$CH_2(L\beta)$ r(23), $C^{\gamma}C^{\delta}$(L2) s(11), $C^{\alpha}C$(L) s(10), CH_2(G) r(7), CN(LG) s(6)
825 MW	820 VW	823	$C^{\delta}ND$(P) d(18), $CH_2(P\delta)$ r(13), $CH_2(P\beta)$ r(12), CO(P) ib(8), $C^{\alpha}C^{\beta}$(P) s(6), CN(PL) s(6)
766 W	764 MW	787	ND_2 r(27), CN(T) s(24), $C^{\alpha}C$(G) s(22), CO(G) s(5)

TABLE 3 (continued)

Observed[a]		Calc.	Potential energy distribution[b]
Raman	i.r.		
	740 W	744	CO(P) ob(33), CO(L) ib(7)
733 W		718	CO(L) ib(14), CH_2(Pδ) r(10)
		706	$C^{\alpha}ND$(P) d(17), $C^{\delta}ND$(P) d(12), $C^{\alpha}C^{\beta}$(P) s(8), C^{β}(P) b1(7)
	690 W,b	685	CH_2(Pβ) r(22), $C^{\gamma}C^{\delta}N$(P) d(17), $C^{\beta}C^{\gamma}C^{\delta}$(P) d(11), $C^{\alpha}NC^{\delta}$(P) d(11), CH_2(G) r(6), CO(P) ib(6)
		669	CO(G) ib(18), $C^{\alpha}C$(G) s(15), CO(L) ob(13), ND_2 r(7), $NC^{\alpha}C$(G) d(5), ND_2 w(5), CN(LG) t(5)
	646 W	655	$C^{\alpha}C^{\beta}C^{\gamma}$(P) d(18), C^{β}(P) b2(14), $C^{\alpha}NC^{\delta}$(P) d(10), $C^{\alpha}C^{\beta}C^{\gamma}$(P) d(7), CO(L) ob(6), $C^{\alpha}CN$(P) d(5)
		650	CH_2(Pγ) r(18), CO(L) ob(11), CO(P) ob(9), $C^{\alpha}ND$(P) d(9), $C^{\alpha}C$(P) s(7), CO(P) ib(6), CH_2(Pδ) r(6)
	624 MW	637	CN(T) t(29), ND_2 w(17), CO(L) ob(14)
		626	CO(L) ob(38), CN(T) t(16), $C^{\alpha}C$(G) s(7), CO(G) ib(7)
	577 VW	570	$C^{\alpha}CN$(L) d(14), $C^{\alpha}CN$(G) d(10), $NC^{\alpha}C$(L) d(9), CO(G) ib(9), ND_2 w(6)
	554 VW	552	CH_2(Pγ) r(22), CH_2(Pδ) r(14), CH_2(Pβ) r(11), $C^{\beta}C^{\gamma}C^{\delta}$(P) d(11), $C^{\gamma}C^{\delta}N$(P) d(10), $C^{\alpha}C$(P) s(5), $C^{\alpha}ND$(P) d(5)
548 VW	548 VW	547	ND_2 w(42), CN(T) t(29), ND . . . O(TX) d(26), CO(G) ob(11)
520 VW	520 W	516	CN(PL) t(55), ND(L) ob(39), ND . . . O(L) d(20)
488 W		480	$C^{\alpha}CN$(G) d(21), CN(PL) t(13), CO(G) ib(9), $C^{\alpha}C^{\beta}C^{\gamma}$(L) d(8), ND(L) ob(6), $NC^{\alpha}C$(G) d(6), CH_2(Lβ) b2(5)
450 VW		456	CN(LG) t(62), ND(G) ob(22), ND . . . O(G) d(18), CN(PL) t(7), C^{γ}(L) sd(7)
		432	CO(G) ob(60), C^{γ}(L) sd(9), ND . . . O(TX) d(7), ND(G) ob(6), CN(LG) t(5)
421 W		421	CO(G) ob(25), CN(LG) t(24), C^{γ}(L) sd(23), ND(G) ob(21), ND . . . O(G) d(11), CH_2(G) w(7), $NC^{\alpha}C$(G) d(6)
401 W		391	C^{γ}(L) sd(27), C^{γ}(P) b2(16), C^{γ}(P) b1(7), $C^{\alpha}C^{\beta}C^{\gamma}$(L) d(7), CO(L) ib(7)

TABLE 3 (continued)

Observed[a]		Calc.	Potential energy distribution[b]
Raman	i.r.		
		379	C^{γ}(P) b2(37), C^{γ}(P) b1(17), C^{β}(L) b1(8), ND(G) ob(6)
346 VW		349	O . . . D(L) s(40), C^{γ}(P) b1(11), $C^{\alpha}CN$(L) d(6)
		330	O . . . D(L) s(50), C^{β}(P) b2(7), CNC^{α}(L) d(6)
		319	O . . . D(PX) s(71)
313 W		307	$NC^{\alpha}C$(P) d(14), CO(P) ib(14), O . . . D(PX) s(12), C^{β}(P) b1(7), C^{β}(P) b2(5), CNC^{α}(L) d(5)
		301	C^{β}(P) b1(19), O . . . D(G) s(10), C^{β}(L) b2(8), $NC^{\alpha}C$(G) d(7), CNC^{α}(L) d(6)
		291	O . . . D(G) s(75), $C^{\alpha}CN$(G) d(6)
289 MS		279	C^{γ}(P) b1(23), $C^{\gamma}C^{\delta}$(L2) t(11), $C^{\gamma}C^{\delta}$(L1) t(8), $NC^{\alpha}C$(G) d(6), C^{β}(L) b1(6)
277 VW		266	$NC^{\alpha}C$(G) d(15), C^{γ}(P) b2(11), $NC^{\alpha}C$(L) d(10), CO(L) ib(9), ND(G) ob(9), CO(P) ob(6)
		254	$C^{\alpha}CN$(P) d(18), C^{β}(L) b1(18), CNC^{α}(L) d(10), ND(G) ob(8), O . . . D(PX) s(6)
		245	$C^{\gamma}C^{\delta}$(L1) t(61), $C^{\gamma}C^{\delta}$(L2) t(37)
		235	$C^{\gamma}C^{\delta}$(L2) t(44), $C^{\gamma}C^{\delta}$(L1) t(26)
		219	$C^{\alpha}CN$(L) d(24), CNC^{α}(L) d(11), C^{γ}(P) b1(8), $C^{\alpha}CN$(P) d(7)
		208	N . . . D(P) s(50), $NC^{\alpha}C$(G) d(8)
		203	N . . . D(P) s(35), $NC^{\alpha}C$(G) d(10), ND(G) ob(5)
		191	$C^{\gamma}C^{\delta}$(P) t(10), C^{β}(P) b1(9), $NC^{\alpha}C$(L) d(8), $C^{\gamma}C^{\delta}N$(P) d(7), $C^{\beta}C^{\gamma}$(P) t(7), $C^{\alpha}CN$(L) d(7), $C^{\beta}C^{\gamma}C^{\delta}$(P) d(6), CNC^{α}(L) d(5)
		146	$C^{\alpha}N$ . . . D(P) d(30), $C^{\delta}N$ . . . D(P) d(12), CNC^{α}(P) d(9), D . . . O(L) s(8), C^{β}(L) b1(5)
		143	$C^{\delta}N$ . . . D(P) d(29), $C^{\alpha}N$ . . . D(P) d(15), D . . . O(L) s(7), D . . . O(T) s(6)
		130	D . . . O(P) s(51), D . . . O(T) s(7), $C^{\delta}N$ . . . D(P) d(7)
		128	D . . . O(G) s(65)
		123	D . . . O(G) s(18), D . . . O(T) s(16), D . . . O(P) s(14), $C^{\delta}N$ . . . D(P) d(6), ND(L) ob(5)
		116	D . . . O(L) s(29), D . . . O(T) s(19), $C^{\delta}N$ . . . D(P) d(10), $C^{\alpha}N$ . . . D(P) d(9), D . . . O(P) s(6), DN . . . D(P) d(6)
		115	D . . . O(P) s(15), O . . . D(PI) s(13), $C^{\alpha}N$ . . . D(P) d(11), C^{β}(L) b2(10),

TABLE 3 (continued)

Observed[a]		Calc.	Potential energy distribution[b]
Raman	i.r.		
			$C^{\alpha}C^{\beta}C^{\gamma}$(L) d(9), ND(L) ob(6), D . . . O(T) s(5)
		112	D . . . O(L) s(33), D . . . O(T) s(11), CNC^{α}(P) d(9), NC^{α}(P) t(6)
		105	CO(G) t(54), O . . . D(PI) s(9), D . . . O(T) s(8)
		97	CO(L) t(56), O . . . D(PI) s(5)
		89	CO(G) t(23), CO(L) t(20), O . . . D(PI) s(15)
		82	$C^{\alpha}C^{\beta}$(P) t(8), $C^{\beta}C^{\gamma}$(L) t(7), CO(L) t(6), $NC^{\alpha}C$(P) d(5), ND . . . O(L) d(5)
		73	CO . . . D(L) d(14), ND . . . O(TX) d(10), ND . . . O(G) d(8), CO . . . D(G) d(8), ND(L) ob(8), ND_2 w(7), $NC^{\alpha}C$(L) d(6), CO(L) t(5), CN(T) t(5)
		70	CO . . . D(G) d(27), ND(TX) t(17), ND . . . O(L) d(7)
		68	ND(G) ob(19), CO . . . D(G) d(18), CO . . . D(L) d(9), ND . . . O(G) d(7), $C^{\alpha}C$(G) t(7), CO(G) t(5)
		60	ND . . . O(TX) d(27), ND_2 w(19), CN(T) t(15), CO . . . D(L) d(7), NC^{α}(G) t(6)
		51	CO . . . D(L) d(17), CO . . . D(G) d(14), ND . . . O(P) d(13), $C^{\beta}C^{\gamma}$(L) t(10), $C^{\alpha}C$(P) t(6), ND(L) ob(6)
		45	CO . . . D(L) d(36), CN(LG) t(17), $C^{\beta}C^{\gamma}$(L) t(17), ND . . . O(G) d(16), ND(G) ob(8)
		43	$C^{\beta}C^{\gamma}$(L) t(20), CO . . . D(L) d(6), CO . . . D(G) d(6), ND(G) ob(6), CNC^{α}(P) d(6)
		41	ND . . . O(P) d(15), CO . . . D(PI) d(15), $C^{\alpha}C$(P) t(10), $C^{\alpha}C$(G) t(10), ND(TX) t(9), $C^{\alpha}C^{\beta}$(L) t(6)
		36	CO . . . D(PX) d(94)
		34	$C^{\alpha}C^{\beta}$(L) t(42), $C^{\beta}C^{\gamma}$(L) t(21), ND . . . O(G) d(5), ND(G) t(5)
		30	ND . . . O(L) d(26), CN(PL) t(10), ND . . . O(P) d(9), O . . . D(PI) s(7), NH(TX) t(6)
		28	$C^{\alpha}C$(G) t(22), ND(TX) t(21), ND(L) ob(14), ND(TI) t(7)
		25	CO(P) t(21), ND(L) t(21), ND(G) t(18), ND(L) ob(7), $C^{\alpha}C^{\beta}$(L) t(6)
		24	CO(P) t(54), ND(G) t(24)
		24	ND(L) t(61), $C^{\alpha}C^{\beta}$(L) t(16)

TABLE 3 (continued)

Observed[a]		Calc.	Potential energy distribution[b]
Raman	i.r.		
		22	ND(G) t(24), CO(P) t(17), ND(L) ob(15), $C^{\alpha}C$(P) t(8), NC^{α}(L) t(8), C^{β}(L) b1(6), ND . . . O(L) d(5)
		20	NC^{α}(G) t(35), $C^{\alpha}C$(L) t(16), ND . . . O(G) d(14), ND(G) ob(7)
		16	$C^{\alpha}C$(P) t(40), ND . . . O(P) d(8), O . . . D(PI) d(8), NC^{α}(G) t(8)
		11	ND(P) t(18), $C^{\alpha}C$(L) t(15), NC^{α}(G) t(10), CO . . . D(PI) d(9), ND(TI) t(8), ND . . . O(TI) d(7), $C^{\alpha}C$(P) t(7), NC^{α}(L) t(7), ND(G) ob(7)
		8	ND(P) t(68), $C^{\alpha}C$(P) t(13)

[a] S = strong, M = medium, W = weak, V = very, sh = shoulder, b = broad.

[b] s = stretch, as = antisymmetric stretch, ss = symmetric stretch, b = angle bend, ib = in-plane angle bend, ob = out-of-plane angle bend, w = wag, r = rock, t = torsion, d = deformation, sd = symmetric deformation, tw = twist, L = leucine, G = glycine, P = proline, T = terminal. Numbers 1 and 2 following L refer to $C^{\delta}1$ and $C^{\delta}2$ of leucine respectively. X refers to external and I refers to intra. In O . . . D and D . . . O the first atom belongs to the residue in bracket and the second atom is either an intramolecular or an externally added atom. In the case of ND . . . O and CO . . . D the group CO or ND belongs to the residue in the bracket. Only contributions of 5% or greater are included.

[c] Unperturbed frequency.

β-turn tetrapeptide (4) and a type II β-turn cyclic tripeptide (6). On *N*-deuteration a number of changes occur. Of course, the 1556 cm^{-1} band disappears, as does the NH_2 bend mode at 1615 cm^{-1}. The contribution of the terminal CN(T) stretch to the latter mode is predicted to shift to 1509 cm^{-1}, and a weak new absorption is indeed seen here. The moderate CN(LG) stretch contribution to the 1545 cm^{-1} mode is predicted to shift to 1484 cm^{-1}, similar to the case of poly(glycine I) (21) and β-poly(L-alanine) (22). Its combination with some ND(G) in-plane-bend may make the calculated frequency 10–20 cm^{-1} higher (21, 22); if so, an assignment to the 1457 S cm^{-1} i.r. band may not be too unreasonable, in spite of the poor frequency agreement. This would be consistent with the enhanced intensity in the 1427 MS cm^{-1} i.r. band, which is associated with CN(PL) stretch plus NC^{α}(P) stretch, particularly since there is no change in character of the CH_2 and CH_3 modes in this region. It is true that the CH_2(G) bend mode is predicted to shift from 1453 to 1437 cm^{-1}, but since it is not particularly strong to begin with (unless it is contributing to the 1451 VS cm^{-1} Raman band, which decreases somewhat in relative intensity in the *N*-deuterated molecule), we do not feel that it should be assigned to the 1427 MS cm^{-1} i.r. band.

The CH deformation and amide III regions are reasonably well accounted for, although some subtle as well as large changes occur on *N*-deuteration. For example, calculated modes at 1479, 1477, 1458, 1454, 1451, 1447, 1396, 1383, 1282, and 1244 cm^{-1} hardly change their character or frequency, and can be well correlated in the two spectra. The 1391, 1375, and 1300 cm^{-1} modes alter slightly, dropping by ~6 cm^{-1}, but can probably still be assigned as before. The other modes are significantly altered by the disappearance of NH_2 or NH

bend, resulting in a significant redistribution of internal coordinate contributions. Thus, the region between 1380 and 1300 cm^{-1} is affected by the loss of NH_2 and NH bend contributions from the modes at 1354 and 1328 cm^{-1}. The CH_2(G) wag contributions from these two and the 1335 cm^{-1} mode coalesce in a purer mode predicted at 1342 cm^{-1}, and assignable to observed Raman bands at 1350 M or 1341 M cm^{-1}. We choose the former assignment because we do not expect, by analogy with the hydrogenated molecule, to correlate a strong Raman band with the (relatively unaltered) 1369 cm^{-1} mode, and also because it is not unreasonable to expect that the newly predicted 1316 cm^{-1} mode could have a comparable intensity Raman counterpart to the observed 1334 MS cm^{-1} i.r. band. (The frequency agreement here is admittedly poor, but it must be remembered that force fields have been transferred without refinement.) The disappearance of the 1271 MS cm^{-1} Raman band is clear-cut, nor is a counterpart expected at this position for the *N*-deuterated molecule. On the other hand, our calculation shows that the disappearance on *N*-deuteration of the 1241 cm^{-1} Raman (S) and i.r. (M) band is only partly due to its having a small NH in-plane bend component; mostly it is a result of a redistribution of coordinate contributions in the normal modes. A new band is predicted at 1228 cm^{-1} in the *N*-deuterated molecule, with a contribution from $C^{\delta}ND(P)$ deformation (which may be why the frequency agreement is so poor); this may be part of the reason for the altered modes. These results stress two important points: amide III modes are particularly sensitive to side chain composition and other backbone vibrations (1, 2, 31); and *N*-deuteration can cause frequency and intensity changes in modes that have very small contributions from NH in-plane bend. Conversely, no frequency and only small intensity changes on *N*-deuteration occur in bands with NH in-plane bend if, as is the case with the 1244 cm^{-1} mode, there is a very large contribution from another internal coordinate, in this case CH_2 twist.

The region between 1200 and 700 cm^{-1} is quite complex, since it contains skeletal stretch as well as side chain deformation modes. Although *N*-deuteration shifts help in the analysis, because of the large number of NH_2 and NH modes in this region and the complex redistribution when these are changed to ND_2 and ND, some of the assignments must be considered tentative. Nevertheless, the calculations predict many features of the spectra quite well. Some modes retain their essential character on *N*-deuteration, and their assigned Raman and i.r. bands are recognizable in both spectra; this is the case for those modes calculated at 1168, 1109, 1079, 1012, 988, 892, and 843 cm^{-1}. In some cases modes of generally similar character that are absent (or present) in the spectra of the hydrogenated molecule appear (or disappear) in those of the *N*-deuterated molecule; modes calculated at 1154 and 979 cm^{-1} (and 1196 and 853 cm^{-1}) are in this category. All of the main bands that disappear on *N*-deuteration, and therefore should contain NH_2 or NH deformation, are well predicted; these are the calculated modes at 1134 (NH_2 rock), 982 ($C^{\delta}NH(P)$ deformation), 921 and 885 ($C^{\alpha}NH(P)$ and $C^{\delta}NH(P)$ deformation), 877 and 751, 739 (NH_2 wag), and 802 ($C^{\alpha}NH(P)$ deformation) cm^{-1}. In some cases the ND contribution gives rise to a recognizably new band; examples are modes at 1097 (ND_2 bend), 1019 (ND(G) in-plane bend), 932 (ND_2 rock and ND(G) in-plane bend), 854 ($C^{\alpha}ND(P)$ and $C^{\delta}ND(P)$ deformation), 823 ($C^{\delta}ND(P)$ deformation), and 787 (ND_2 rock) cm^{-1}. In other cases, however, its mixing with existing modes causes only frequency shifts or intensity changes; this seems to be the case for modes at 1048 (shifting to 1051 and 1048), 1032 (to 1019), and 974 and 963 (which coalesce to 956 and 947) cm^{-1}. It should be noted that some observed bands seem to change hardly at all on *N*-deuteration, but in fact they are replaced by quite different modes at about the same frequency; examples of these are bands at 1165 MW (i.r.), 1130 W (i.r.), 1041 M (R) and 1038 W (i.r.), 976 W (R and i.r.), 957 M (R), and 920 M (i.r.) cm^{-1}.

The region of the amide V mode (NH out-of-plane bend plus CN torsion) for a model type II β-turn has been predicted (2) to be about 650–570 cm^{-1}. In the present structure it might be expected that there would be two such modes, associated with the Pro-Leu and Leu-Gly peptide groups. In fact the calculation predicts that contributions from NH out-of-plane bend

occur in four bands, calculated at 699, 657, 603, and 575 cm^{-1}. Four observed bands that disappear on *N*-deuteration can indeed be identified in the i.r. spectrum, thus clearly demonstrating the power of the normal mode technique. The highest frequency band is outside the previously indicated range (2), but this may be due to the particular structure of this β-turn. (Also, the 657 cm^{-1} mode has only a small NH out-of-plane bend, and no CN torsion, contribution, making it, strictly speaking, not an amide V mode.) The modes containing ND out-of-plane bend are quite weak, and are difficult to assign with certainty although observed bands are found.

A detailed study has not been made of the region below 500 cm^{-1} in the i.r. or below 250 cm^{-1} in the Raman. Those modes not involving primarily H . . . O stretch (which is not expected to be realistically reproduced by the present calculation) are reasonably well assigned, although detailed confirmation awaits further study. A significant redistribution of internal coordinates occurs as a result of the new contributions of D motions in the *N*-deuterated molecule.

CONCLUSIONS

Our normal mode calculations on the crystalline Pro-Leu-Gly-NH_2 structure show that we can meaningfully reproduce the observed i.r. and Raman bands of this type II β-turn. The average discrepancy between observed and calculated frequencies below 1700 cm^{-1} is 6 cm^{-1}, which is comparable to that for the standard polypeptide chain structures (21, 22, 32), and very good considering that the force field was transferred without refinement. (Of the above 68 modes for which there are observed bands, the distribution of these discrepancies is as follows: 0–4 cm^{-1} –30, 5–9 cm^{-1} –22, 10–19 cm^{-1} – 14, over 20 cm^{-1} –2.) Beyond just frequency agreement we of course also predict correctly those modes that contain NH and NH_2 contributions and therefore shift on *N*-deuteration. Thus, for example, the deuteration shift of one of the amide I modes can be understood on the basis of its having a small NH_2 bend component without having to postulate a change in conformation (11). The normal mode calculations also show that there are four bands having NH out-of-plane bend contributions, although from the structure we might expect only two amide V modes. Such predictive capability demonstrates the importance of normal mode calculations in analyzing the conformation of peptides from vibrational spectroscopy, and provides a sound base for studying the solution conformations of this peptide (Naik, V.M. & Krimm, S., to be published).

ACKNOWLEDGMENTS

This research was supported by National Science Foundation grants PCM-7921652 and DMR-7800753. V.M.N. is grateful for fellowship support from the Macromolecular Research Center.

REFERENCES

1. Bandekar, J. & Krimm, S. (1979) *Proc. Natl. Acad. Sci. US* **76**, 774–777
2. Krimm, S. & Bandekar, J. (1980) *Biopolymers* **19**, 1–29
3. Venkatachalam, C.M. (1968) *Biopolymers* **6**, 1425–1436
4. Bandekar, J. & Krimm, S. (1979) in *Peptides: Structure and Biological Function.* Proceedings of the Sixth American Peptide Symposium (Gross, E. & Meienhofer, J., eds.), pp. 241–244, Pierce Chemical Co., Rockford, IL
5. Bandekar, J. & Krimm, S. (1980) *Biopolymers* **19**, 31–36
6. Maxfield, F.R., Bandekar, J., Krimm, S., Evans, D.J., Leach, S.J., Némethy, G. & Scheraga, H.A. (1981) *Macromolecules* **14**, 997–1003
7. Bandekar, J., Evans, D.J., Krimm, S., Leach, S.J., Lee, S., McQuie, J.R., Minasian, E., Némethy, G., Pottle, M.S., Scheraga, H.A., Stimson, E.R. & Woody, R.W. (1982) *Int. J. Peptide Protein Res.* **19**, 187–205
8. Celis, M.E., Taleisnik, S. & Walter, R. (1971) *Proc. Natl. Acad. Sci. US* **68**, 1428–1433
9. Nair, R.M.G., Kastin, A.J. & Schally, A.V. (1971) *Biochem. Biophys. Res. Commun.* **43**, 1376–1381
10. Reed, L.L. & Johnson, P.L. (1973) *J. Am. Chem. Soc.* **95**, 7523–7524
11. Hseu, T.H. & Chang, H. (1980) *Biochim. Biophys. Acta* **624**, 340–345
12. Fox, J.A., Tu, A.T., Hruby, V.J. & Mosberg, H.J. (1981) *Arch. Biochem. Biophys.* **211**, 628–631
13. Higashijima, T., Tasumi, M. & Miyazawa, T. (1975) *FEBS Lett.* **57**, 175–178

14. Hruby, V.J., Brewster, A.I. & Glasel, J.A. (1971) *Proc. Natl. Acad. Sci. US* **68**, 450–453
15. DesLauriers, R., Walter, R. & Smith, I.C.P. (1973) *FEBS Lett.* **37**, 27–32
16. Schwartz, R.W., Mattice, W.L. & Spirtes, M.A. (1979) *Biopolymers* **18**, 1835–1848
17. Naik, V., Bandekar, J. & Krimm, S. (1980) *Proceedings of the VIIth International Conference on Raman Spectroscopy*, (Murphy, W.F., ed.), pp. 596–597, North-Holland, Amsterdam
18. Hsu, S.L., Moore, W.H. & Krimm, S. (1975) *J. Appl. Phys.* **46**, 4185–4193
19. Moore, W.H. & Krimm, S. (1976) *Biopolymers* **15**, 2439–2464
20. Moore, W.H. & Krimm, S. (1976) *Biopolymers* **15**, 2465–2483
21. Dwivedi, A.M. & Krimm, S. (1982) *Macromolecules* **15**, 177–185
22. Dwivedi, A.M. & Krimm, S. (1982) *Macromolecules* **15**, 186–193; (1983) *Macromolecules* **16**, 340
23. Johnston, N.H. (1975) Ph.D. Dissertation, University of Michigan
24. Schachtschneider, J.H. & Snyder, R.G. (1963) *Spectrochim. Acta* **19**, 117–168
25. Uno, T., Machida, K. & Saito, Y. (1969) *Bull. Chem. Soc. Japan* **42**, 897–904
26. Uno, T., Machida, K. & Saito, Y. (1971) *Spectrochim. Acta* **27A**, 833–844
27. Krimm, S. & Abe, Y. (1972) *Proc. Natl. Acad. Sci. US* **69**, 2788–2972
28. Moore, W.H. & Krimm, S. (1975) *Proc. Natl. Acad. Sci. US* **72**, 4933–4935
29. Pouchert, C.J. (1975) *The Aldrich Library of Infrared Spectra*, 2nd edn. Aldrich Chemical Co., Milwaukee, WI
30. Krimm, S. & Dwivedi, A.M. (1982) *J. Raman Spectroscopy* **12**, 133–137
31. Hsu, S.L., Moore, W.H. & Krimm, S. (1976) *Biopolymers* **15**, 1513–1528
32. Dwivedi, A.M. & Krimm, S. (1983) *Biopolymers*, in press

Address:

Professor *S. Krimm*
Biophysics Research Division
University of Michigan
2200 Bonisteel Boulevard
Ann Arbor, MI 48109
USA